

Oxygen vacancies in N doped anatase TiO₂: Experiment and first-principles calculations

Abdul K. Rumaiz,^{1,a)} J. C. Woicik,² E. Cockayne,² H. Y. Lin,³ G. Hassnain Jaffari,⁴ and S. I. Shah^{3,4}

¹National Synchrotron Light Source, Brookhaven National Laboratory, Upton, New York 11973, USA

²National Institute of Standards and Technology, Gaithersburg, Maryland 20899, USA

³Department of Materials Science and Engineering, University of Delaware, Newark, Delaware 19716, USA

⁴Department of Physics and Astronomy, University of Delaware, Newark, Delaware 19716, USA

(Received 28 October 2009; accepted 16 November 2009; published online 31 December 2009)

We have determined the electronic and atomic structure of N doped TiO₂ using a combination of hard x-ray photoelectron spectroscopy and first-principles density functional theory calculations. Our results reveal that N doping of TiO₂ leads to the formation of oxygen vacancies and the combination of both N impurity and oxygen vacancies accounts for the observed visible light catalytic behavior of N doped TiO₂. © 2009 American Institute of Physics. [doi:10.1063/1.3272272]

Titanium dioxide (TiO₂) is widely studied for applications such as photocatalysis,^{1,2} photovoltaics,³ and dilute magnetic semiconductor.^{4,5} One of the most promising applications of TiO₂ is its catalytic capability of splitting water into oxygen and hydrogen.⁶ However, due to its large bandgap (3 and 3.2 eV for rutile and anatase, respectively), pure TiO₂ is only activated by ultraviolet light, lowering the efficiency of its catalytic process. Doping of TiO₂ can introduce energy levels in the bandgap,^{7,8} effectively tailoring its electronic structure to absorb light in the visible region. Recently N doped TiO₂ has been synthesized and its catalytic properties demonstrated with visible light.^{9,10} This success, however, is riddled with controversies concerning the electronic structure of N doped TiO₂. Asahi *et al.*¹¹ have proposed a bandgap narrowing due to the lower binding energy of the N 2*p* relative to the O 2*p* levels, while Valentin *et al.*¹² have proposed a localized dopant N 2*p* state just above the O 2*p* valence band maximum. While optical absorption measurements of N doped TiO₂ have shown bandgap reduction,^{10,13,14} the corresponding change in the valence band has not been observed by photoemission.¹⁵ Although photoemission on N doped TiO₂ has been extensively studied by several groups,^{15,16} the role of oxygen vacancies has not been sufficiently addressed. Here we have studied the electronic structure of well characterized N-doped TiO₂ prepared by reactive pulsed laser deposition using hard x-ray photoelectron spectroscopy. The experimental data are compared¹⁷ with theoretical calculations of the density of states (DOS) for TiO₂ with N doping both with and without oxygen vacancies. Together, the data and theory demonstrate that N doping produces O vacancies in TiO₂.

Experiments were performed at the National Synchrotron Light Source using the National Institute of Standards and Technology beam line X24A. The double-crystal monochromator was operated with Si(111) crystals, and high-resolution photoelectron spectra were obtained with a hemispherical electron analyzer. The photon energy was calibrated prior to each measurement by the Fermi level of a standard Ag foil. Anatase TiO₂ with about 7 % N doping was synthesized on Si substrates using reactive pulsed laser depo-

sition. Details of the synthesis are described elsewhere.^{14,18}

Figure 1(a) shows the Ti 2*p* core level for both pure and N doped TiO₂ plotted versus electron kinetic energy. The peaks labeled 1 and 2 are the 2*p*_{3/2} and 2*p*_{1/2} spin orbit split contributions to the Ti 2*p* core line from Ti⁴⁺.¹⁸ In the case of the N doped sample, we observe two extra peaks labeled 3 and 4. This spectrum is quite similar to that obtained from TiO₂ reduced by Ar⁺ sputtering, and the peak position la-

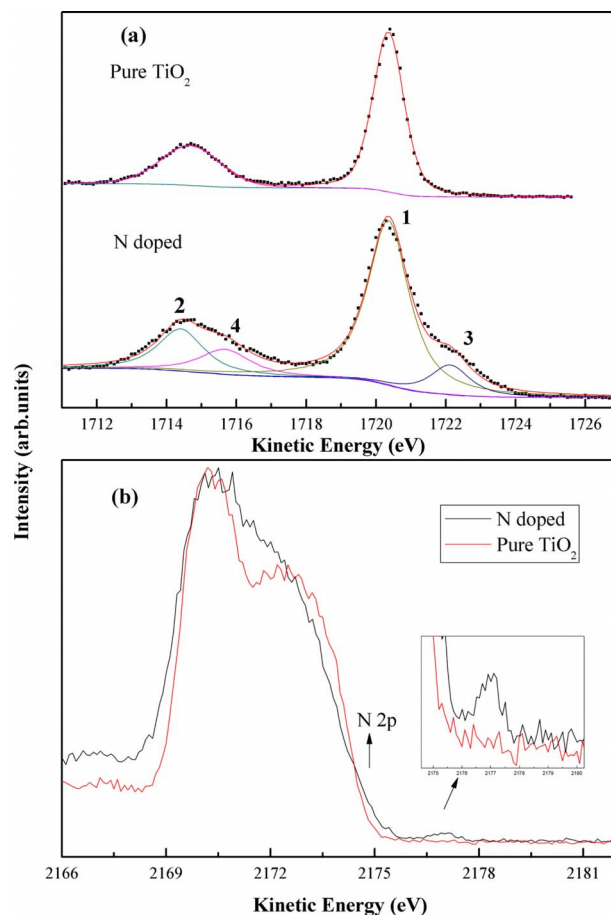


FIG. 1. (Color online) (a) Ti 2*p* core level for N doped and pure anatase TiO₂. (b) Valence-band spectra of N doped and pure anatase TiO₂. The inset shows the magnified region of the occupied state within the gap.

^{a)}Electronic mail: rumaiz@bnl.gov.

beled 3 is very close to the reported values for Ti^{3+} relative to Ti^{4+} .¹⁵ It must be noted that all of our measurements were obtained without Ar^+ etch as afforded by the relatively high excitation photon energy. The additional peaks observed in the spectrum have been attributed to Ti^{3+} induced by the formation of N-Ti-O bonds,¹⁹ but Nambu *et al.*¹⁵ have also questioned this conclusion. Based on the relative peak positions of the third and fourth peak we conclude that the N doping of the TiO_2 produces Ti^{3+} ions.

The valence-band spectra recorded at photon energy $h\nu = 2178$ eV is shown in Fig. 1(b) for both pure and N doped TiO_2 . The positions of the curve were adjusted by aligning the Ti^{4+} 2*p* core level. This allows us to quantitatively compare the change in bandgap reported by others to the change in valence band, presuming the conduction band is unaffected by N doping.¹¹ Due to its formal Ti^{4+} oxidation state, pure TiO_2 primarily has a filled O 2*p* derived valence band separated from an empty Ti 3*d*, 4*s*, and 4*p* derived conduction band by a bulk bandgap of 3.2 eV.²⁰ The valence-band spectra show the emission from the O 2*p* band, and visual examination reveals two features in the N doped sample as follows: a tailing of the valence-band maximum to higher kinetic energy and an impurity state just above this maximum compared to undoped TiO_2 . The tail-like state is attributed to the N 2*p* level since the binding energy of N 2*p* is less than O 2*p* thus extending the valence-band maximum to lower binding energy. However, the shift observed in the valence band (of about 0.3 eV) is not enough to explain the observed redshift observed in optical absorption spectra reported (of about 0.5–0.8 eV) by several groups.^{10,13,14}

To understand the likely structures produced by N doping of TiO_2 , we performed density functional theory calculations for pure anatase and anatase with various defects using the VASP package.²¹ The calculations used projector augmented wave pseudopotentials,²² with 12 valence electrons for Ti, 6 for O, and 5 for N. The local density approximation (LDA) was used for the exchange-correlation functional. A plane-wave cutoff energy of 353 eV was used with an augmentation charge cutoff of 1500 eV. DOS calculations were performed on a $\sqrt{2} \times \sqrt{2} \times 1$ anatase supercell with 8 Ti and 16 O for pure anatase. Relaxation of cells and atomic positions were performed using 32 k-points in the full Brillouin zone, and DOS calculations were then performed using 192 k-points. Because the LDA underestimates the cell volume of anatase, calculations were performed under an artificial negative pressure that reproduces the experimental volume. Four structures were studied; (0,0), (1,0), (0,1), and (1,1), where the first number refers to the number of O \rightarrow N substitutions and the second number to the number of O vacancies per 24 atom supercell. One N substitution (6.25%) is close to the experimental value. For the (1,1) cell, each possible interdefect geometry was tested. Formation energies of the defects were calculated, with respect to anatase, O_2 gas, and N_2 gas as “endmember” compounds. The calculated formation energies are (0,1)+6.2 eV; (1,0)+5.5 eV; (1,1)+8.8 eV to +9.7 eV. Importantly, to form an oxygen vacancy in the presence of a nitrogen substitution (+3.3 to +4.2 eV, depending on location) is easier than to form an O vacancy in pure TiO_2 (+6.2 eV). The most favorable geometries found for the N-substitution/ Ti^{3+} /O vacancy complexes are shown in Fig. 2. In Fig. 2(b), the O vacancy is on the octahedral vertex opposite from the N. In Fig. 2(c), two

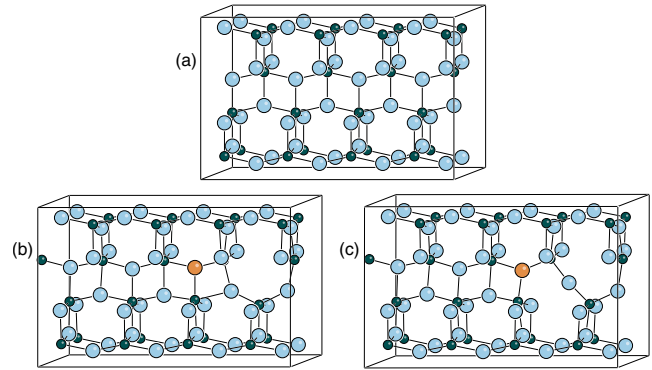


FIG. 2. (Color online) (a) Structure of pure anatase; (b) N/ Ti^{3+} /O vacancy defect complex with O opposite N; (c) “Merging” of two O into central position. In (b) and (c), the Ti^{3+} ion is obscured from this viewpoint.

O positions “merge” into one, resulting in an O that is only twofold coordinated with unusually short Ti—O bonds (0.177 to 0.181 nm), and the cell has significantly larger (about 0.01 nm³) volume. Calculations on larger cells confirm that these two geometries have the lowest energies, and the ordering of their energies changes in going from the LDA volume to the experimental volume.

The resulting DOS curves convolved with a Gaussian of width 0.4 eV to simulate experiment are shown in Fig. 3. The figure shows the calculated DOS for pure, N doped, and N doped plus oxygen vacant TiO_2 . (Weighted over different geometries by the Boltzmann factor). N substitution leads to a tailing of states near the conduction band edge. Only when O vacancies are also present is there an impurity state at the Fermi energy.

To compare theory and experiment, we have followed the discussion of Ref. 17 and constructed the theoretical photoemission DOS curves as the cross-section weighted sum of the angular momentum resolved partial DOS of each atom of the unit cell [see Figs. 4(a) and 4(b)]. This process accounts for the presence of the N dopants, the formation of O vacancies, and the chemical hybridization in the solid-state electronic structure.^{17,23–25} As in Ref. 17, the cross sections were taken from Ref. 26. Figures 5(a) and 5(b) show the comparison between the theoretical and experimental curve for pure and N doped TiO_2 . Curves are plotted setting the Fermi level to be equal to zero. (Experimental Fermi level was obtained

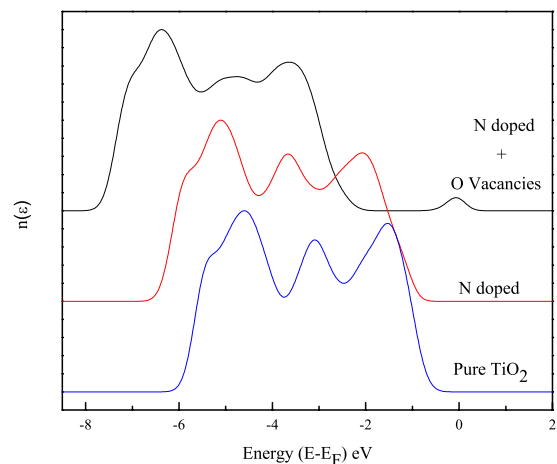


FIG. 3. (Color online) Theoretical electronic structures for pure, N doped, and N doped plus O vacant TiO_2 .

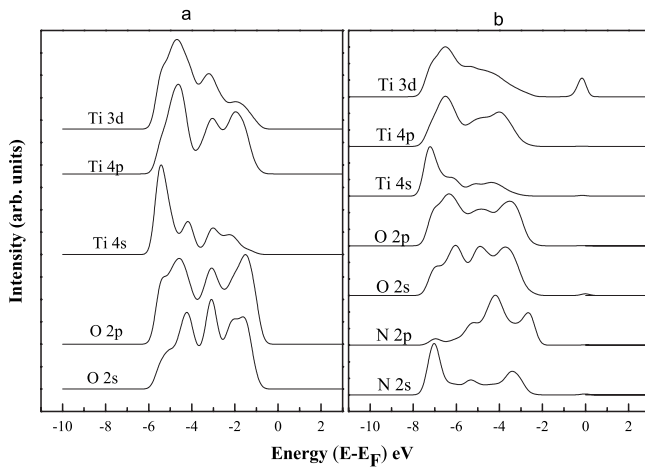


FIG. 4. (a) Theoretical angular-momentum resolved components of Ti, O for pure TiO₂. (b) Theoretical angular-momentum resolved components of Ti, O, and N for N doped TiO₂ with oxygen vacancies. The curves are normalized with respect to the maximum in each case.

by collecting the VB spectra of a standard Ag foil.) The defect level near the Ti 3d edge is confirmed as an occupied Ti 3d level both experimentally and theoretically.

The formation of O vacancy related defect level also explains the knee formation in the optical absorbance spectra of N doped TiO₂ reported by several authors.^{10,13,14} The absorbance tail close to 500 nm^{13,14} could be due to the acceptor level above the valence-band maximum. The experimentally measured VB shows vacancy related defect level at about 1 eV above the valence-band maximum. This agrees well with some of the reported bandgap reductions as a result of high concentration of N doping in TiO₂. Earlier UPS measurements on Ar⁺ sputtered TiO₂ have shown the position and amplitude of this defect state depend on the amount of the oxygen vacancies or surface reduction.²⁰ From the foregoing discussions we have now demonstrated that these defect levels are responsible for the change in bandgap. We note that the theoretical calculations do not quantitatively reproduce the bandgap and the exact bandgap reduction due to following two effects: (1) the LDA bandgap error (2.4 eV computed for pure anatase versus 3.2 eV experimentally) and (2) relatively poor theoretical treatment of Ti 3d electron correlations. For the latter, preliminary LDA+U calculations

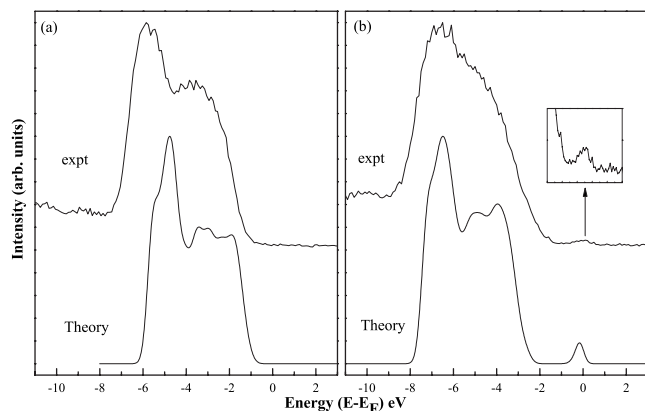


FIG. 5. (a) Theoretical DOS and the experimental valence band for pure anatase TiO₂. (b) Theoretical DOS and the experimental valence band for N doped anatase TiO₂. The curves have been scaled to equal peak height.

show better localization of the occupied Ti 3d states and a lowering of the energies of these states from near the conduction-band minimum to near the valence-band maximum as U increases from 0 to 8 eV.

In conclusion, we have shown that N doping in anatase TiO₂ leads to the formation of oxygen vacancies. The electronic structure is modified, and we directly observe the occupied Ti 3d states near the Fermi level. The valence-band structure shows tailing to lower binding energies due to the incorporation of less tightly bound N 2p level which is hybridized with O 2p level causing a reduction in bandgap. However, the shift is not large enough to account for the change in bandgap reported from earlier work. Thus the combination of N impurity and the O vacancy is responsible for the UV-vis absorption response in the visible region as well as the visible catalytic activity of N doped TiO₂.

A.K.R would like to acknowledge P.D. Siddons (NSLS) for support. This work was performed at the National Synchrotron Light Source, which is supported by the U.S. Department of Energy.

¹A. L. Linsebigler, G. Lu, and J. T. Yates, Jr., *Chem. Rev. (Washington, D.C.)* **95**, 735 (1995).

²*Photocatalytic Purification and Treatment of Water and Air*, edited by D. Ollis and H. Al-Ekabi (Elsevier, Amsterdam, 1993).

³B. O'Regan and M. Gratzel, *Nature (London)* **353**, 737 (1991).

⁴T. Diel, H. Ohno, M. Matsukura, J. Cibert, and D. Ferrand, *Science* **287**, 1019 (2000).

⁵R. Janisch and N. A. Spaldin, *Phys. Rev. B* **73**, 035201 (2006).

⁶A. Fujishima and K. Honda, *Nature (London)* **37**, 238 (1972).

⁷S. I. Shah, W. Li, C.-P. Huang, O. Jung, and C. Ni, *Proc. Natl. Acad. Sci. U.S.A.* **99**, 6482 (2002).

⁸W. Li, A. I. Frenkel, J. C. Woicik, C. Ni, and S. I. Shah, *Phys. Rev. B* **72**, 155315 (2005).

⁹S. Sakthivel and H. Kisch, *ChemPhysChem* **4**, 487 (2003).

¹⁰H. Irie, Y. Watanabe, and K. Hashimoto, *J. Phys. Chem.* **107**, 5483 (2003).

¹¹R. Asahi, T. Morikawa, T. Ohwaki, K. Aoki, and Y. Taga, *Science* **293**, 269 (2001).

¹²C. Di Valentin, G. Pacchioni, and A. Selloni, *Phys. Rev. B* **70**, 085116 (2004); J. Y. Lee, J. Park, and J.-H. Cho, *Appl. Phys. Lett.* **87**, 011904 (2005).

¹³K. Kobayakawa, Y. Murakami, and Y. Sato, *J. Photochem. Photobiol., A* **170**, 177 (2005).

¹⁴H. Y. Lin, A. Rumaiz, M. Schultz, C. P. Huang, and S. I. Shah (unpublished).

¹⁵A. Nambu, J. Graciani, J. A. Rodriguez, Q. Wu, E. Fujita, and J. F. Sanz, *J. Chem. Phys.* **125**, 094706 (2006).

¹⁶M. Batzill, E. H. Morales, and U. Diebold, *Phys. Rev. Lett.* **96**, 026103 (2006).

¹⁷J. C. Woicik, E. J. Nelson, L. Kronik, M. Jain, J. R. Chelikowsky, D. Heskett, L. E. Berman, and G. S. Herman, *Phys. Rev. Lett.* **89**, 077401 (2002).

¹⁸A. K. Rumaiz, B. Ali, A. Ceylan, M. Boggs, T. Beebe, and S. I. Shah, *Solid State Commun.* **144**, 334 (2007).

¹⁹F. Esaka, K. Furuya, H. Shimada, M. Imamura, N. Matsubayashi, H. Sato, A. Nishijima, A. Kawana, H. Ichimura, and T. Kikuchi, *J. Vac. Sci. Technol. A* **15**, 2521 (1997).

²⁰V. E. Henrich and P. A. Cox, *The Surface Science of Metal Oxides*, 1st ed. (Cambridge University Press, Cambridge, 1994).

²¹G. Kresse and J. Joubert, *Phys. Rev. B* **59**, 1758 (1999).

²²P. E. Blochl, *Phys. Rev. B* **50**, 17953 (1994).

²³Z. Zhang, S.-P. Jeng, and V. E. Henrich, *Phys. Rev. B* **43**, 12 004 (1991).

²⁴R. Heise, R. Courths, and S. Witzel, *Solid State Commun.* **84**, 599 (1992).

²⁵L. D. Finkelstein, E. Z. Kurmaev, M. A. Korotin, A. Moewes, B. Schneider, S. M. Butorin, J.-H. Guo, J. Nordgren, D. Hartmann, M. Neumann, and D. L. Ederer, *Phys. Rev. B* **60**, 2212 (1999).

²⁶M. B. Trzhaskovskaya, V. I. Nefedov, and V. G. Yarzhemsky, *At. Data Nucl. Data Tables* **77**, 97 (2001).